Modulated photoabsorption in strained $Ga_{1-x}In_xAs/GaAs$ multiple quantum wells

I. Sela, D. E. Watkins, B. K. Laurich, and D. L. Smith
Los Alamos National Laboratory, Los Alamos, New Mexico 87545

S. Subbanna* and H. Kroemer
Department of Electrical and Computer Engineering, University of California at Santa Barbara, Santa Barbara, California 93106
(Received 19 November 1990)

Modulated photoabsorption measurements in strained $Ga_{1-x}In_xAs/GaAs$ multiple quantum wells are presented. The modulating intensities vary from a few to about 10^5 W/cm^2. The absorption near the first heavy-hole exciton is probed with a tunable Ti:sapphire laser. The modulating beam is either from the same Ti:sapphire laser as the test beam or from an Ar^+-ion laser whose photon energy is much larger than the first heavy-hole exciton transition energy. A dramatic difference is observed in the modulated transmission spectra for the two modulating wavelengths. This difference in behavior can be explained as arising from screening of the residual surface electric field by Ar^+-ion-laser excitation but not by Ti:sapphire laser excitation. The Ar^+-ion laser creates high-energy carriers that are initially free to drift in the surface field before they are captured in the quantum wells. Carriers excited by the low-photon-energy Ti:sapphire laser are created in the quantum wells and therefore cannot effectively screen the surface field. We present a model based on surface-field screening and exciton saturation for Ar^+-ion-laser modulation and exciton saturation alone for Ti:sapphire laser modulation that describes the observed results.

I. INTRODUCTION

The optical properties of the strained-layer $Ga_{1-x}In_xAs/GaAs$ materials system have received considerable attention.[1-10] Strain splits the heavy- and light-hole bands and, therefore, excitonic transitions involving these bands are usually well separated spectrally. In one sense, this spectral separation of corresponding heavy- and light-hole transitions simplifies optical studies of $Ga_{1-x}In_xAs/GaAs$ compared to optical studies of $GaAs/Ga_{1-x}Al_xAs$ in which corresponding heavy- and light-hole transitions are spectrally close. In this paper we present an experimental study of modulated photoabsorption near the first heavy-hole exciton in $Ga_{1-x}In_xAs/GaAs$ multiple quantum wells (MQW). The modulating intensities used in the study vary from a few to about 10^5 W/cm^2. The absorption is probed with a spectrally tunable beam from a Ti:sapphire laser. The modulating beam is either from the same Ti:sapphire laser as the test beam (and therefore has the same wavelength as the test beam) or from an Ar^+-ion laser whose photon energy is much larger than the first heavy-hole exciton transition energy. For the case in which the modulating beam is from the Ti:sapphire laser, an electron-hole pair created by absorption of the modulating beam is confined in a $Ga_{1-x}In_xAs$ quantum well. For the case in which the modulating beam is from the Ar^+-ion laser, electrons and holes created by absorption of the modulating beam have a higher energy than the GaAs barriers so that they are initially free to move throughout the quantum structure. Subsequently, these electrons and holes lose energy and become confined in the quantum wells.

We observe a dramatic difference between the modulated transmission spectra using the two different modulating wavelengths. Modulation with the Ti:sapphire laser leads to increased transmission (reduced absorption) at the exciton resonance for all modulation intensities. These results are well described by saturation of the excitonic transition[11-14] and can be parametrized by a single saturation intensity over a wide intensity range. Very different behavior is observed for modulation with the Ar^+-ion laser. At modulation intensities below a few kW/cm^2 (the precise value is sample dependent), modulation with the Ar^+-ion laser leads to reduced transmission (increased absorption), whereas at higher modulating intensities, it leads to increased transmission. At modulation intensities greater than several kW/cm^2, modulation with the Ar^+-ion laser shows only the same exciton saturation as does modulation with the Ti:sapphire laser.

We attribute the different behavior observed at the two modulating wavelengths to screening of surface electric fields by the electrons and holes generated by the Ar^+-ion laser. These surface electric fields arise because the energy bands at the surface are at a different position, relative to the Fermi energy, than they are deeper in the structure. This band bending corresponds to the surface electric fields. They are the same fields responsible for modulated photoreflectance.[15-18] The surface fields shift the excitonic transition to the red and decrease the strength of the excitonic transitions by increasing the spatial separation of the electron and hole wave functions in the quantum well. The electrons and holes created by Ar^+-ion-laser modulation screen the surface fields because these carriers are created at energies higher than the GaAs barriers. This allows them to move freely in

response to the surface fields until they lose energy and are captured in the quantum wells. The fields are not effectively screened by electron-hole pairs generated by Ti:sapphire laser modulation because each electron-hole pair is generated in a quantum well and is therefore not free to move in response to the field. Screening of the surface fields by Ar^+-ion-laser modulation increases the strength of the excitonic transition and shifts the transition energy to the blue, as compared to the case with unscreened fields. Thus, screening tends to reduce transmission (increase absorption) at the exciton resonance. Surface-field screening saturates as the carrier density increases, so the usual exciton saturation effect dominates the modulated transmission spectra for both Ar^+-ion and Ti:sapphire laser modulation at high intensity. We present modulated transmission spectra of $Ga_{1-x}In_xAs/GaAs$ multiple quantum wells using both Ar^+-ion and Ti:sapphire laser modulation over a wide intensity range. A model based on surface-field screening and exciton saturation for Ar^+-ion-laser modulation and exciton saturation alone for Ti:sapphire laser modulation that describes the observed results is presented.

The paper is organized as follows: Our experimental approach is described in Sec. II, results of the optical measurements are presented in Sec. III, Sec. IV contains a discussion of the theoretical model, and our results are summarized in Sec. V.

II. EXPERIMENTAL APPROACH

MQW samples were grown by molecular-beam epitaxy on semi-insulating GaAs substrates with 0.1-μm undoped GaAs buffer layers. There were 30 undoped periods in the MQW's, each consisted of a 7-nm $Ga_{1-x}In_xAs$ well and a 14-nm GaAs barrier. A 30-nm undoped GaAs cap layer completed the structure. Four samples were studied: two with indium concentration given by $x=0.12$ (samples 1) and two with indium concentration $x=0.17$ (samples 2). For each concentration one sample was grown along the [100] crystal axis and the other was grown along the [211]B crystal axis.[19] Corresponding samples were grown simultaneously to obtain similar structures. Rutherford backscattering measurements were used to determine the In concentrations. Photoluminescence measurements taken at very low optical intensity show a strong, sharp peak associated with the 1hh exciton. No peaks associated with extrinsic bound excitons were observed. We measured the free carrier recombination time by using a picosecond optical (532-nm) excitation source to generate the carriers while monitoring the change in sample transmission at the exciton resonance using a cw Ti:sapphire laser beam and a fast photodiode. In all four samples the change in transmission induced by the picosecond laser pulse had a decay constant of about 2 ns. All transmission measurements were made after the samples had been mechanically polished with a 5° wedge between the surfaces to eliminate interference effects.

Three types of measurements were made: transmission as a function of wavelength, differential transmission as a function of test-beam wavelength and both test- and pump-beam intensity, and differential photoreflectance. All of the measurements were made with the samples at low temperature (~ 5 K) to avoid heating effects by the cw laser beams. Two experimental approaches were used (Fig. 1). Figure 1(a) shows the usual pump-probe approach in which the Ti:sapphire laser beam is split into a pump and a probe (or test) beam. Figure 1(b) shows a variation on this approach where the Ar^+-ion laser which is used to pump the Ti:sapphire laser is also used for the pump beam. (In another variation a HeNe laser was used to pump the sample.) This figure also shows the setup for the differential photoreflectance measurement. In all cases the two laser beams were focused onto the same spot on the sample and spatial overlap was verified visually using a microscope and an infrared viewer. The spot size of the pump beam was kept bigger than that of the test beam. Spot size was determined using a razor blade mounted on a differential micrometer stage with 1-μm resolution. The razor-blade edge was located at the focal plane of the lens and in front of a power meter that collected the whole laser beam. The diameter for 10% to 90% of full power transmission was 40 μm for the Ti:sapphire pump beam and 20 μm for the test beam. The two laser beams were chopped at different frequencies. The change in test-beam transmission due to the pump-beam modulation was measured using a Si photodiode at D_3 and a lock-in amplifier at the sum of the two chopper frequencies. This approach suppresses scattered light and photoluminescence. Photodiodes at positions D_1 and D_2 were used to monitor input signal intensities after the laser beams were attenuated by neutral density filters. The additional detector D_4 in Fig. 1(b) was used

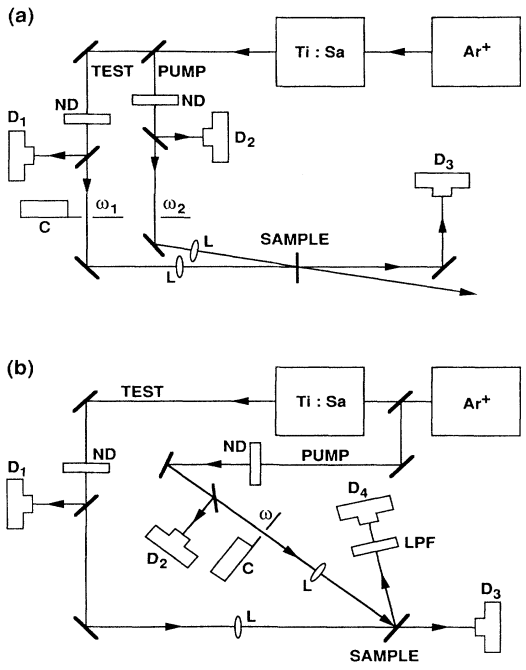

FIG. 1. Schematic of experimental setup for (a) Ti:sapphire laser modulation and (b) Ar^+-ion-laser modulation.

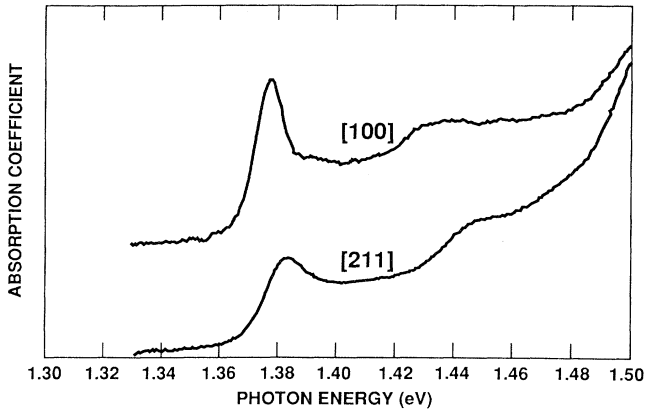

FIG. 2. Measured absorption spectra for the [100] and [211] oriented samples.

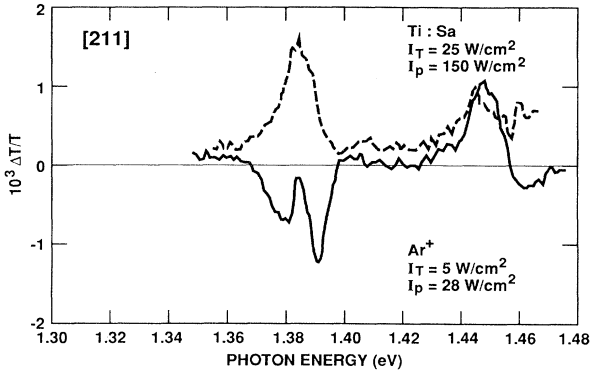

FIG. 4. Low-intensity modulated transmission spectra for the [211] sample with Ti:sapphire laser modulation (dotted line) and Ar^+-ion-laser modulation (solid line).

for photoreflectance measurements. A low-pass optical filter was placed in front of D_4 to block the scattered light from the Ar^+-ion-laser beam. Quoted incident intensities were corrected for reflection at the cryostat windows and the sample front surface.

III. EXPERIMENTAL RESULTS

Figure 2 shows the results of absorption measurements on samples 2. The peaks near 1.38 eV are caused by the 1hh exciton, and the shoulders near 1.44 eV are related to the 1lh exciton. The absorption increases sharply above 1.5 eV because of the GaAs substrate. Results from samples 1 are qualitatively similar to samples 2 for all the measurements and will not be shown here.

Normalized differential transmission measurements for the [100] and [211] samples are shown in Figs. 3 and 4, respectively. These measurements were made with low pump- and test-beam intensities. In both figures, the dashed curve was measured using the Ti:sapphire laser for the pump [Fig. 1(a)] and the solid curve was measured using the Ar^+-ion laser for the pump beam [Fig. 1(b)].

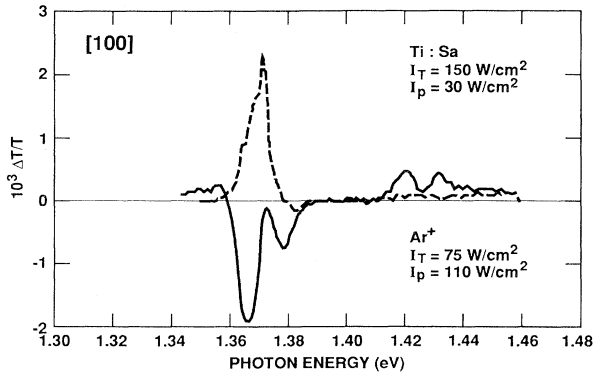

FIG. 3. Low-intensity modulated transmission spectra for the [100] sample with Ti:sapphire laser modulation (dotted line) and Ar^+-ion-laser modulation (solid line).

Measurements made with a HeNe pump laser gave similar results to the Ar^+-ion pump laser. The peaks near 1.38 eV in Figs. 3 and 4 are clearly due to the 1hh exciton (see Fig. 2). The change in signal phase for the two pump wavelengths indicates the existence of more than one mechanism for inducing a change in transmission. The

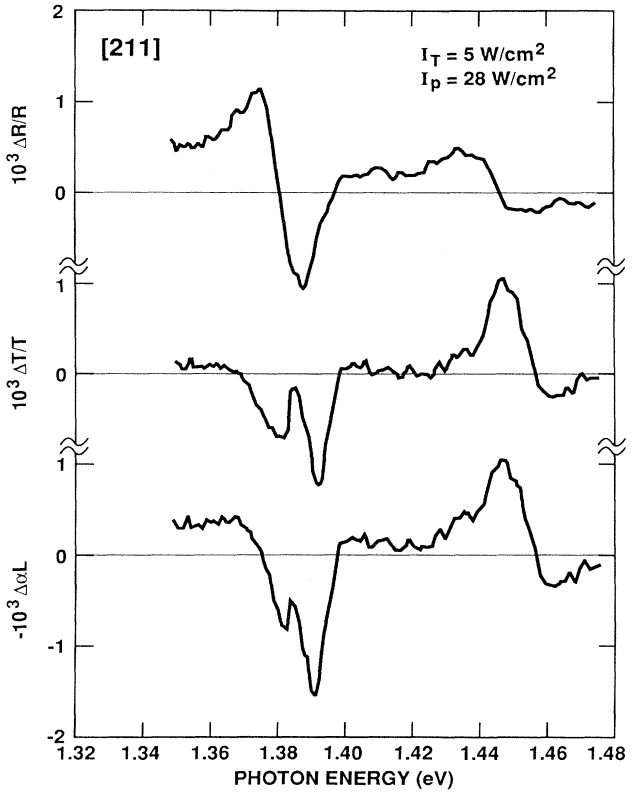

FIG. 5. Low-intensity modulated reflectivity spectrum (upper panel) and modulated transmission spectrum (central panel) for the [211] sample with Ar^+-ion-laser modulation. The modulated absorption spectrum (lower panel) is calculated from the measured reflectivity and transmission spectra.

positive signal indicates a decrease in exciton absorption and is the usual observation in similar experiments.[11] In this case the mechanism is exciton saturation caused by phase-space filling (PSF).[11–14] The negative signal indicates an increase in exciton absorption in the presence of the pump beam. This additional effect is the result of surface-field screening.

Figure 5 shows the results of simultaneous measurements of the differential photoreflectance (upper trace) and the differential transmission (middle trace) for the [211] sample. These measurements were made at low intensity with the Ar^+-ion-laser pump beam. The corrected change in differential absorption signal is shown in the lower trace (see the Appendix). The correction tends to reduce the double negative peaks to a single negative peak, giving a clearer indication of the increase in absorption when the pump beam is incident on the sample. similar results were obtained for the [100] sample.

The change in transmission for the [100] sample at high pump- and test-beam intensities is shown in Fig. 6. Both the Ti:sapphire and Ar^+-ion pump-beam results are displayed in the figure. The signal for the high-intensity resonant pumping case (lower part of the figure) is qualitatively the same as for low-intensity resonant pumping case. The signal for the high-intensity Ar^+-ion pump beam (upper part of Fig. 6) has changed phase relative to the low-intensity result in Fig. 3. The behavior shown in Fig. 6 is consistent with the exciton saturation mechanism independent of pump-beam wavelength.

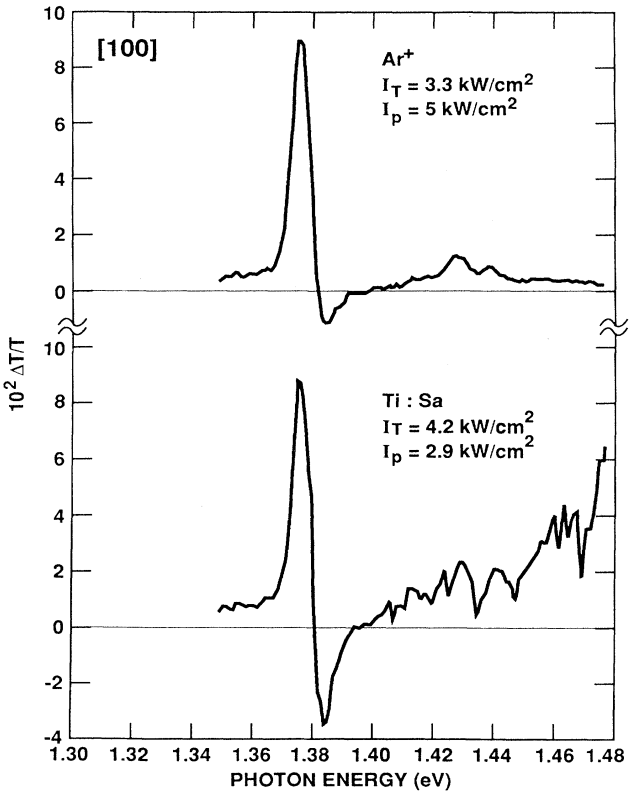

FIG. 6. High-intensity modulated transmission spectra of the [100] sample with Ar^+-ion-laser modulation (upper panel) and Ti:sapphire laser modulation (lower panel).

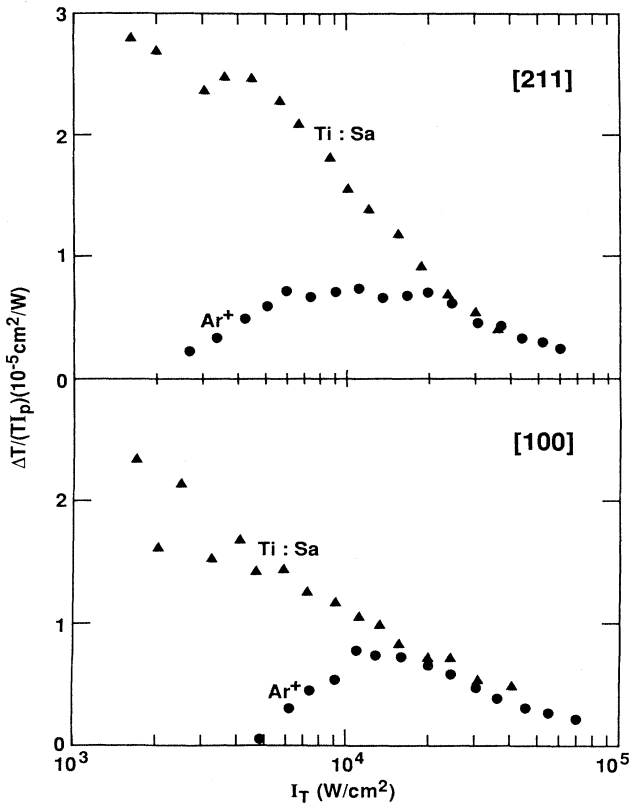

FIG. 7. Normalized modulated transmission for the [211] sample (upper panel) and the [100] sample (lower panel) over a large intensity range with a Ti:sapphire laser (triangle) and an Ar^+-ion laser (circles). The test-beam wavelength is at the peak of the first heavy-hole exciton transition.

The difference between the two pump-beam wavelengths was further examined by measuring the magnitude of the differential transmission signal as a function of the pump intensity for a test-beam wavelength fixed at the peak of the 1hh transition. In this experiment we maintained a ratio of pump-beam intensity to test-beam intensity of 0.1. Figure 7 presents the normalized differential transmission divided by the pump-beam intensity as a function of the test-beam intensity. A clear difference is observed in the results for the two pump-beam wavelengths at low intensities. The data associated with Ti:sapphire pumping are the anticipated results for saturation of a two-level excitonic system. The data associated with Ar^+-ion-laser pumping show a second modulation mechanism that dominates at low intensity.

IV. THEORETICAL MODEL

The absorption spectrum for the [100] multiple-quantum-well structure shown in Fig. 2 has two major features: the 1hh exciton transition at about 1.378 eV

and the 1lh exciton at about 1.435 eV. The [211] sample behaves qualitatively similar to the [100] sample (Ref. 19). The principal modulation effects occur at the 1hh exciton absorption, so we concentrate on describing that transition.

At low intensity and without the presence of an electric field, the multiple-quantum-well absorption coefficient can be written as

$$\alpha(\omega)=\frac{4\pi\omega}{C\sqrt{\epsilon_\infty}}\mathrm{Im}[\chi(\omega)]\ , \tag{1a}$$

where

$$\mathrm{Im}[\chi(\omega)]=\sum_B \frac{e^2}{m^2\omega^2(b+d)}\sum_{e,h}|\langle U_e|\hat{\eta}\cdot\mathbf{P}|U_h\rangle|^2\left[\sum_{n=0}^{\infty}\frac{1}{\pi a^2(n+\frac{1}{2})^3}\left[\frac{\hbar/T_2}{(\varepsilon_n-\hbar\omega)^2+(\hbar/T_2)^2}\right]+\frac{\mu_\parallel}{2\pi\hbar^2}\left[\frac{2}{1+e^{-\beta/\gamma}}\right]\{\pi/2+\tan^{-1}[(\hbar\omega-\varepsilon_B)T_2/\hbar]\}\right]\ , \tag{1b}$$

$$\beta=\pi\left[\frac{\hbar^2}{2\mu_\parallel a^2\varepsilon_B}\right]^{1/2}\ , \tag{1c}$$

and

$$\gamma=\begin{cases}(\hbar\omega-\varepsilon_B)/\varepsilon_B, & \hbar\omega>\varepsilon_B\\ 0, & \hbar\omega<\varepsilon_B\ .\end{cases} \tag{1d}$$

Here, ϵ_∞ is the high-frequency dielectric constant; B sums over the band-to-band transitions with transition energy ε_B; β and γ are terms that appear in the Sommerfeld enhancement factor; b and d are the thickness of the quantum well and barrier, respectively; U_e and U_h are the zone-center wave function for the electron and hole, respectively; the sum on e,h accounts for band-edge degeneracies; $\hat{\eta}$ is the photon polarization vector; $\mathbf{P}$ is the momentum operator; the sum on n is over bound exciton ground and excited states with transition energy ϵ_n; a is the exciton Bohr radius; T_2 is a lifetime broadening factor; and $\mu_\parallel$ is the reduced effective mass for carrier motion in the quantum well. Broadening of multiple-quantum-well optical spectra is usually caused by inhomogeneity, not by lifetime effects. Thus, in principle, a small lifetime broadening should appear in Eq. (1b) and the result should be convolved with a Gaussian to describe this inhomogeneous broadening. However, we are not interested in a detailed line-shape analysis and we simply chose T_2 to give the observed full width at half maximum of the transition. The calculated absorption spectrum is shown in Fig. 8. The parameters used in the calculation are given in Table I.

The effect of exciton saturation can be described by a two-level model.[11,12] We divide the bound-state contribution in Eq. (1b) by $(1+I/I_s)$, where I is the incident optical intensity and I_s is a saturation parameter. We use a single value of I_s for all the ground- and excited-state bound exciton transitions. The excited bound exciton states for a given band-to-band transition make a very weak contribution to the absorption spectrum and a more careful treatment of their saturation properties is not warranted unless a very detailed line-shape analysis were attempted. We concentrate on describing the modulation of the 1hh transition and choose I_s by comparing with the observed results for this transition. We do not separately fit a saturation intensity to the 1lh transition and, as a result, we do not describe the modulation of that transition as well as the 1hh transition.

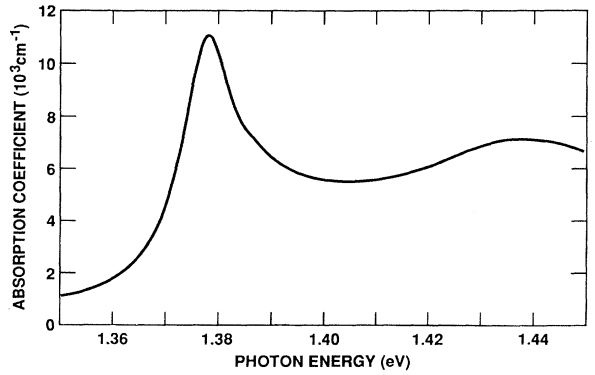

FIG. 8. Calculated absorption coefficient as a function of photon energy at low intensity.

TABLE I. Parameters used in the calculation.

ε_B (eV)	1.386
$\lvert P\rvert^2$ (eV)	18.0
$\mu_\parallel(m_0)$	0.07
$\hbar/T_2$ (meV)	6.0
ε_{ex} (meV)	8.0
a_{ex} (Å)	175.0
c (eV cm^2/V^2)	2×10^{-12}
d (eV cm^2/V^2)	3×10^{-9}
I_s (W/cm^2)	2.5×10^4
E_0 (V/cm)	7500
τ_R (ns)	2
τ_c (ps)	2
μ (cm^2/V s)	400

The surface fields are caused by surface charge, which results from Fermi-level pinning, and compensating space charge in the quantum-well structure. From the growth conditions, we expect that the quantum-well structure is lightly p type (low 10^{15} cm^{-3}) because of carbon incorporation. As a simple model, we take a uniform surface field, resulting from a positive sheet of surface charge and a compensating negative sheet of charge, representing the charged-carbon acceptors, whose distances from the surface are the thickness of the quantum-well structure L (about 0.7 μm in this case). If σ_0 is the unscreened sheet charge density, the unscreened surface field is

$$E_0=\frac{4\pi}{\epsilon}\sigma_0 , \tag{2a}$$

where ϵ is the static dielectric constant. If σ is the screening charge, the screened surface field is

$$E=\frac{4\pi}{\epsilon}(\sigma_0-\sigma) . \tag{2b}$$

To model σ, we note that the carriers must be generated by the modulating Ar^+-ion laser and they must be separated by the surface field. We set

$$\sigma=eNl , \tag{3a}$$

where N is the average volume density of electron-hole pairs generated by the laser in the quantum-well structure

$$N=\frac{I_m\tau_R}{\hbar\omega_m L} . \tag{3b}$$

Here I_m is the intensity of the modulating Ar^+-ion laser, $\hbar\omega_m$ is the photon energy from this laser, and τ_R is the carrier recombination lifetime. (The Ar^+-ion laser is completely absorbed in the quantum-well structure.) In Eq. (3a), l is the average distance by which the electron-hole pair is separated by the surface field (Ref. 20):

$$\frac{1}{l}=\frac{1}{\mu E\tau_c}+\frac{1}{L} , \tag{3c}$$

where τ_c is the time for carrier capture in the quantum well and μ is an untrapped carrier mobility for motion along the growth axis of the quantum-well structure. (Because of scattering from the interface potential discontinuities, we expect that μ should be smaller than the usual low-field carrier mobilities in GaAs.) In the experiment, the Ar^+-ion-laser light is absorbed very near the surface. Holes must be transported to neutralize the charged acceptors in the quantum-well structure. Thus, μ and τ_c refer to hole transport and trapping. Solving for E gives

$$E=\frac{[E_0-(x+y)]+\{[E_0-(x+y)]^2+4yE_0\}^{1/2}}{2} , \tag{4a}$$

where

$$x=\frac{e4\pi}{\epsilon}\frac{I_m}{\hbar\omega_m}\tau_R \tag{4b}$$

and

$$y=\frac{L}{\mu\tau_c} . \tag{4c}$$

The screening model described above is clearly simplified, but it contains the essential physical features of the surface-field screening process.

There are several parameters in Eq. (1b) which change their value when an external field is applied, including the exciton binding energies and Bohr radii, the band-to-band transition energies ε_B, and the squared optical matrix elements $|\langle U_e|\hat{\eta}\cdot\mathbf{P}|U_h\rangle|^2$. For the magnitude of fields considered here ($E\leq E_0\sim 10^4$ V/cm), the change in exciton parameters is quite small[21] and the band-to-band transition energy and squared transition matrix elements are quadratically decreasing functions of the applied field.[22] The surface field is not spatially uniform and its nonuniformity leads to a broadening of the optical spectra. We interpret the solution of Eq. (4) as the maximum value of the surface field and take half this solution as the average value of the surface field. We then have

$$\varepsilon_B=\varepsilon_B^0-c(E/2)^2 , \tag{5a}$$

$$\frac{\hbar}{T_2}=\left[\frac{\hbar}{T_2}\right]^0+\frac{c}{2}(E)^2 , \tag{5b}$$

and

$$|\mathbf{P}|^2=(|\mathbf{P}|^2)^0-d(E/2)^2 , \tag{5c}$$

where E is the solution to Eq. (4), $|\mathbf{P}|^2$ is the squared transition matrix element[23] in Eq. (1b), $\hbar/T_2$ is the half-width-at-half-maximum broadening of the transition, and the superscript 0 indicates the value at zero electric field. The coefficients c and d are determined by numerical calculation[22] of the effect of an electric field on quantum-well optical transitions. These values of c and d are listed in Table I. To calculate a modulated absorption spectrum, we choose a test-beam intensity I_t and a pump-beam intensity I_p. Both I_t and I_p contribute to the exciton saturation. When describing Ar^+-ion-laser modulation, I_p contributes to surface-field screening [Eq. (4)], but when describing Ti:sapphire laser modulation, there is no surface-field screening (i.e., $E=E_0$). The absorption coefficient is calculated both with the pump laser on and with it off. Subtracting gives $\Delta\alpha$, the absorption coefficient with the pump beam on minus that with the pump beam off. The parameters used in the calculations are given in Table I. We have chosen parameters to give a qualitative overall description of the data discussed above rather than attempting a detailed fit of the data from a particular sample.

In Fig. 9 we show calculated results for low-intensity modulated absorption ($-\Delta\alpha L$), both including the effect of surface-field screening to describe Ar^+-laser modulation and neglecting the effect of surface-field screening to describe Ti:sapphire laser modulation. The intensities used in the calculation correspond to those in Fig. 4. After the reflection corrections shown in Fig. 5 are taken into account, the calculation gives a reasonable description of the low-intensity modulated absorption spectra.

In Fig. 10 we show calculated results for high-intensity

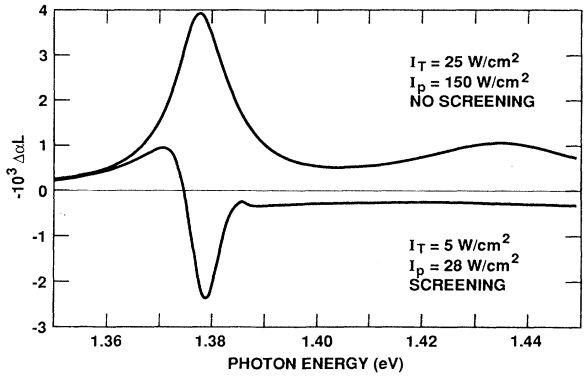

FIG. 9. Calculated absorption modulation spectra, at low modulation intensity, including surface-field screening (lower curve) and neglecting surface-field screening (upper curve).

modulated absorption $(-\Delta\alpha L)$, both including and neglecting the effect of surface-field screening. The intensities used in the calculation correspond to those in Fig. 6. At these high intensities, the effect of surface-field screening has saturated and exciton saturation dominates the modulated photoabsorption spectra. The calculations, including and neglecting the surface screening effect, are essentially the same. There is good correspondence between the calculation shown in Fig. 10 and the experimental spectra shown in Fig. 6.

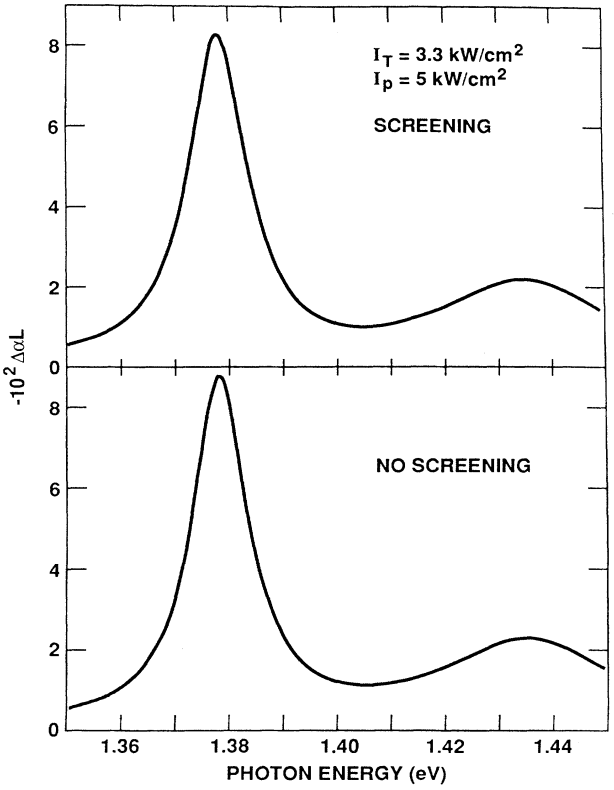

FIG. 10. Calculated absorption modulation spectra, at high modulation intensity, including surface-field screening (upper panel) and neglecting surface-field screening (lower panel).

In Fig. 11 we show calculated results for the normalized modulated absorption over a large intensity range both including and neglecting the effect of surface-field screening. The results in Fig. 11 are calculated at the peak of the 1hh exciton transition (1.378 eV). The pump intensity is 0.1 times the test intensity. The curve calculated neglecting surface-field screening is essentially that describing saturation of a two-level system. The curve calculated including surface-field screening deviates strongly from that neglecting it at low intensities but the two curves largely coincide at high intensities. There is a good correspondence between the calculated results shown in Fig. 11 and the experimental results shown in Fig. 7.

The model described in this section is simplified, but it provides a good description of all the observed results. The parameters used in the calculation are physically reasonable. The transition energies and linewidths were taken from the observed results. The transition matrix element, exciton parameters, effective masses, and electric-field dependence of the transition energy and matrix element were taken from quantum-well electronic-structure calculations.[22] (These parameters were not adjusted to match the experimental results.) The recombination lifetime was measured. The saturation intensity I_s was chosen to fit the exciton saturation observed in the Ti:sapphire modulation experiments. The unscreened surface field E_0 capture time τ_c, and untrapped carrier mobility μ (only the product $\tau_c\mu$ actually enters the model) were chosen to describe the Ar^+-ion modulation experiments. A surface field of 7.5×10^3 V/cm is a typical value. The value 2 ps used for τ_c is consistent with calculations for this trapping time in GaAs/$Ga_{1-x}Al_xAs$ QW.[24] The value 400 cm^2/V s for μ implies a scattering mean free path of about 170 Å (Ref. 25). This is a reasonable value (about one period) for a hole whose energy is above the GaAs valence-band edge (i.e., the hole is not confined by the GaAs barriers) in these structures.

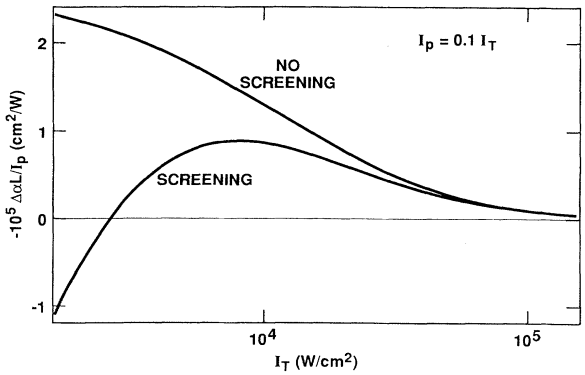

FIG. 11. Calculated normalized absorption modulation including surface-field screening (lower curve) and neglecting surface-field screening (upper curve). The absorption modulation is calculated at the peak of the first heavy-hole exciton.

V. SUMMARY AND CONCLUSIONS

We have presented the results of an experimental study of modulated photoabsorption near the first heavy-hole exciton in $Ga_{1-x}In_xAs/GaAs$ multiple quantum wells in which the modulating intensity was varied from a few to about 10^5 W/cm^2. The absorption was probed with a spectrally tunable beam from a Ti:sapphire laser. The modulating beam was either from the Ti:sapphire laser or an Ar^+ laser. A dramatic difference is observed in modulated transmission spectra using the two different modulating wavelengths. Modulation with the Ti:sapphire laser is well described by saturation of the excitonic transition. Modulation with the Ar^+-ion laser also shows the effect of screening of surface fields in the quantum structure. (Such screening does not occur in Ti:sapphire laser modulation because the electron-hole pairs created by this laser are trapped in the quantum wells.) The surface-field screening significantly changes the modulated absorption spectra. We present a model based on surface-field screening and exciton saturation for Ar^+-ion-laser modulation and exciton saturation alone for Ti:sapphire laser modulation that describes the observed results.

ACKNOWLEDGMENTS

We thank T. E. Mitchell and O. Unal for transmission electron measurements on these samples. The work of two of us (S.S. and H.K.) was supported by the Office of Naval Research.

APPENDIX: REFLECTIVITY CORRECTIONS

In this appendix we describe how the modulated reflectivity and modulated transmission results were combined to give the modulated absorption spectrum shown in Fig. 5. The modulated reflectivity from the front surface of the sample was measured. (Reflections from the cryostat windows and the back surface of the sample were spatially separated from the reflection at the sample front.) The reflected intensity I_R and transmitted intensity I_T can be written as

$$I_R = R_F I_I \tag{A1a}$$

and

$$I_T = (1-R_F)(1-R_B)e^{-\alpha L} I_I \ , \tag{A1b}$$

where I_I is the incident intensity, R_F and R_B are the reflectivities of the front and back surfaces of the sample, and α and L are the absorption coefficient and thickness of the quantum-well structure. The modulated laser changes R_F and α. Expanding to lowest order gives

$$\frac{\Delta I_T}{I_T} = \frac{-\Delta R_F}{(1-R_F)} - \Delta\alpha L \tag{A2a}$$

and

$$\frac{\Delta I_R}{I_R} = \frac{\Delta R_F}{R_F} \ . \tag{A2b}$$

Therefore we have

$$-\Delta\alpha L = \frac{\Delta I_T}{I_T} + \frac{\Delta I_R}{I_R}\left[\frac{R_F}{1-R_F}\right] . \tag{A2c}$$

We used $R_F = 0.3$ in constructing Fig. 5.

*Present address: IBM, East Fishkill, Hopewell Junction, NY 12533.

[1] J. Y. Marzin, M. N. Charasse, and B. Sermage, Phys. Rev. B **31**, 8298 (1985).
[2] I. J. Fritz, B. L. Doyle, T. J. Drummond, R. M. Biefeld, and G. C. Osbourn, Appl. Phys. Lett. **48**, 1606 (1986).
[3] J. Menendez, A. Pinczuk, D. J. Werder, S. K. Sputz, R. C. Miller, D. L. Sivco, and A. Y. Cho, Phys. Rev. B **36**, 8165 (1987).
[4] T. G. Andersson, Z. G. Chen, V. C. Kulakovskii, A. Uddin, and J. T. Vallin, Phys. Rev. B **37**, 4032 (1988).
[5] N. G. Anderson, W. D. Laidig, R. M. Kolbas, and Y. C. Lo, J. Appl. Phys. **60**, 2361 (1986).
[6] G. Ji, D. Huang, U. K. Reddy, T. S. Henderson, R. Houdre, and H. Morkoc, J. Appl. Phys. **62**, 3366 (1987).
[7] S. H. Pan, H. Shen, F. H. Pollak, W. Zhuang, Q. Xu, A. P. Roth, R. A. Masut, C. Lacelle, and D. Morris, Phys. Rev. B **38**, 3375 (1988).
[8] B. K. Laurich, K. Elcess, C. G. Fonstad, J. G. Beery, C. Mailhiot, and D. L. Smith, Phys. Rev. Lett. **62**, 649 (1989).
[9] K. J. Moore, G. Duggan, K. Woodbridge, and C. Roberts, Phys. Rev. B **41**, 1090 (1990).
[10] K. J. Moore, G. Duggan, K. Woodbridge, and C. Roberts, Phys. Rev. B **41**, 1095 (1990).
[11] D. S. Chemla, D. A. B. Miller, P. W. Smith, A. C. Gossard, and W. Wiegmann, IEEE J. Quantum Electron. **QE-20**, 265 (1984).
[12] S. H. Park, J. F. Morhange, A. D. Jeffrey, F. A. Morgan, A. Chavez-Pirson, H. M. Gibbs, S. W. Koch, N. Peyghambarian, M. Derstine, A. C. Gossard, J. H. English, and W. Wiegmann, Appl. Phys. Lett. **52**, 1201 (1988).
[13] R. Zimmermann, Phys. Status Solidi B **146**, 371 (1988).
[14] M. Wegener, I. Bar-Joseph, G. Sucha, M. N. Islam, N. Sauer, T. Y. Chang, and D. S. Chemla, Phys. Rev. B **39**, 12 794 (1989).
[15] H. Shen, P. Parayanthal, F. H. Pollak, M. Tomkiewicz, T. J. Drummond, and J. N. Schulman, Appl. Phys. Lett. **48**, 653 (1986).
[16] B. V. Shanabrook, O. J. Glembocki, and W. T. Beard, Phys. Rev. B **35**, 2540 (1987).
[17] H. Shen, S. H. Pan, F. H. Pollak, and R. N. Sacks, Phys. Rev. B **37**, 10 919 (1988).

[18]O. J. Glembocki and B. V. Shanabrook, Superlatt. Microstruct. **5**, 603 (1989).

[19]Transmission electron microscopy studies of these samples suggest that considerable strain relaxation occurred. Similar samples consisting of 10 MQW periods showed much lower crystal defect densities; see O. Unal, B. K. Laurich, and T. E. Mitchell, *MRS Symposium Proceedings* (Materials Research Society, Pittsburgh, 1990), Vol. 183, pp. 183–186.

[20]The average rate for capture ($1/\tau_c$) and the average rate to traverse the sample ($\mu E/L$) add to give the average rate at which holes are separated from the electrons. Dividing by the average velocity (μE) gives the reciprocal of the average separation ($1/l$).

[21]J. A. Brum and G. Bastard, Phys. Rev. B **31**, 3893 (1985).

[22]See, for example, D. L. Smith and C. Mailhiot, Phys. Rev. Lett. **58**, 1264 (1987).

[23]We define

$$|\mathbf{P}|^2=\frac{2}{m}\sum_{e,h}|\langle U_e|P_x|U_h\rangle|^2 .$$

[24]J. A. Brum and G. Bastard, Phys. Rev. B **33**, 1420 (1986).

[25]We use an effective mass of $0.45m_0$ and an average hole energy of 35 meV (one optical phonon energy) above the GaAs barriers to make this estimate.